Catalysts **2013**, *3*, 247-260; doi:10.3390/catal3010247

OPEN ACCESS

catalysts

ISSN 2073-4344

www.mdpi.com/journal/catalysts

Article

Inactivation of *E. Coli* in Water Using Photocatalytic, Nanostructured Films Synthesized by Aerosol Routes

Jinho Park [1], Eric Kettleson [1,2], Woo-Jin An [1], Yinjie J. Tang [1] and Pratim Biswas [1,*]

[1] Aerosol and Air Quality Research Laboratory, Department of Energy, Environmental and Chemical Engineering, School of Engineering and Applied Science, Washington University in St. Louis, Campus Box 1180, St. Louis, MO 63130, USA; E-Mails: jinhopark@go.wustl.edu (J.P.); emk2@wustl.edu (E.K.); woojinan@wustl.edu (W.-J.A.); yinjie.tang@seas.wustl.edu (Y.J.T.)

[2] Department of Environmental Health, University of Cincinnati, Cincinnati, OH 45267, USA

* Author to whom correspondence should be addressed; E-Mail: pbiswas@wustl.edu; Tel.: +1-314-935-5482; Fax: +1-314-935-5464.

Received: 10 December 2012; in revised form: 13 January 2013 / Accepted: 30 January 2013 / Published: 4 March 2013

Abstract: TiO_2 nanostructured films were synthesized by an aerosol chemical vapor deposition (ACVD) method with different controlled morphologies: columnar, granular, and branched structures for the photocatalytic inactivation of *Escherichia coli* (*E. coli*) in water. Effects of film morphology and external applied voltage on inactivation rate were investigated. As-prepared films were characterized using scanning electron microscopy (SEM), transmission electron microscopy (TEM), X-ray diffractometry (XRD), and UV-VIS. Photocatalytic and photoelectrochemical inactivation of *E. coli* using as-prepared TiO_2 films were performed under irradiation of UVA light (note: UVA has a low efficiency to inactivate *E. coli*). Inactivation rate constants for each case were obtained from their respective inactivation curve through a 2 h incubation period. Photocatalytic inactivation rate constants of *E. coli* are 0.02/min (using columnar films), and 0.08/min (using branched films). The inactivation rate constant for the columnar film was enhanced by 330% by applied voltage on the film while that for the branched film was increased only by 30%. Photocatalytic microbial inactivation rate of the columnar and the branched films were also compared taking into account their different surface areas. Since the majority of the UV radiation that reaches the Earth's surface is UVA, this study provides an opportunity to use sunlight to efficiently decontaminate drinking water.

Keywords: aerosol chemical vapor deposition; photocatalysis; photoelectrochemical inactivation; TiO_2; UVA

1. Introduction

Currently, nearly 20% of the world's population lacks clean drinking water [1,2]. With a rapidly increasing world population, this problem is further exacerbated. Many groundwater and surface water sources are contaminated, thus necessitating safe and reliable disinfection techniques [3]. Conventionally, water is disinfected by chlorination, which uses free chlorine as a strong oxidant [4]. The biggest drawback to this method is the possible production of carcinogenic disinfection by-products (DBPs) such as trihalomethanes and haloacetic acids [5]. Ozone is an alternative strong oxidant for disinfection of water. However, ozonation may also produce toxic DBPs during the disinfection process [6]. Therefore, safe and sustainable alternative water disinfection methods are required.

Photocatalytic disinfection is considered a promising alternative due to several advantages. First, photocatalytic disinfection does not produce any toxic or carcinogenic DBPs. Photocatalytic materials used for disinfection can be recycled while the conventional chemical methods consume chemical disinfectants. In addition, titanium dioxide (TiO_2) is a non-hazardous photocatalytic material. Oxidants generated by such photocatalytic materials are strong enough to inactivate pathogenic microorganisms in water [7].

TiO_2 nanoparticles have been studied extensively as a photocatalytic material for inactivation of pathogenic microorganisms such as bacteria, viruses, algae, and fungi because they have several desirable features: a large surface area, thermal and chemical stability, and they are rather inexpensive [8–13]. Matsunaga *et al.* [8] first reported photocatalytic inactivation of microorganisms. They inactivated *Lactobacillus acidophilus*, *Saccharomyces cerevisiae* and *E. coli* using a TiO_2 particle suspension. Wei *et al.* [9] used P25 (TiO_2, Degussa) to inactivate *E. coli* in water. They reported effects of particle dosage, light intensity *etc.* on the inactivation rate. Hu *et al.* [10,11] have synthesized Ag/TiO_2 and $Ag/AgBr/TiO_2$ composites to inactivate bacteria under irradiation with visible light. However, TiO_2 nanoparticles must overcome a number of challenges before replacing conventional water disinfection methods. First, TiO_2 nanoparticles must be removed from disinfected water post-treatment. Unfortunately, removing nano-sized particles from liquid is very difficult and energy intensive. Secondly, particle suspensions in water can block light, an essential shading effect during microbial photoactivation [12]. In addition, inactivation efficiency is low because electron-hole (e-h) pairs generated by photoactivation recombine rapidly [7,14].

To overcome these problems, several research groups have studied inactivation of pathogenic microorganisms using immobilized TiO_2 films [15–18]. Photocatalytic inactivation using an immobilized TiO_2 film alleviates post-treatment removal of nanoparticles and reduces light blockage. Kuhn *et al.* [16] reported inactivation of *E. coli*, *Pseudomonas aeruginosa* (*P. aeriginosa*), *Staphylococcus aureus* (*S. aureus*), *Enterococcus faecium* (*E. faecium*) and *Candida albicans*

(*C. albicans*) using P25-coated glass under UV light. They investigated susceptibility of the bacteria, which was shown as follows: *E. coli* > *P. aeriginosa* > *S. aureus* > *E. faecium* > *C. albicans*. Sunanda *et al.* [17] also investigated inactivation of *E. coli* using a dip-coated TiO_2 film. To enhance inactivation rates, Reddy *et al.* [18] prepared TiO_2 coated on zeolite for use in inactivation of *E. coli*.

Recently, a few research groups have studied photoelectrochemical inactivation by applying an electric potential on the TiO_2 film to effectively separate electron-hole (e-h) pairs to reduce their recombination rate [10,19]. Yu *et al.* [19] prepared a Ti-based photocatalytic film by electrodeposition and investigated the photoelectrochemical inactivation of *E. coli* by applied voltage on the film. Heyden *el al.* [20] also studied both photocatalytic and photoelectrochemical inactivation of *E. coli* using a quantum dot-deposited TiO_2 nanotube film.

When using TiO_2 films for photocatalytic and photoelecrochemical reactions, the morphology of the TiO_2 film is a determinant factor, which influences photogenerated electron mobility [21]. However, the effect of the morphology of the film on efficiency of photocatalytic inactivation of microorganism has not been systemically studied. In this paper, inactivation of a microorganism using TiO_2 films with different morphologies is reported. *E. coli* was selected as the model species in this study because it is a representative indicator of contamination of water [14]. Several morphological TiO_2 films were synthesized via the aerosol chemical vapor deposition (ACVD) method [22,23]. This study describes the effect of three TiO_2 film morphologies (columnar, granular, and branched structures) on the efficiency of inactivation of *E. coli* in water. In addition, the effect of applied voltage on the photocatalytic inactivation is also investigated.

2. Experimental Section

2.1. Preparation and Characterization of TiO_2 Films by ACVD

TiO_2 films with different morphologies were prepared using the ACVD method. Titanium tetraisopropoxide (TTIP, Sigma-Aldrich, St. Louis, MO, USA) was used as a precursor for the synthesis of the films. Tin-doped indium oxide (ITO) coated aluminosilicate glass (Delta Technologies, Stillwater, MN, USA) was selected as a substrate for the deposition of the TiO_2 films. Synthesis of TiO_2 films via the ACVD method has been described by An *et al*. [22,23]. Process parameters for each morphology—columnar, granular, and branched structures—are summarized in Table 1.

Table 1. Summary of experimental parameters for synthesis of TiO_2 films via aerosol chemical vapor deposition (ACVD).

Test	Morphology	Temperature of substrate (°C)	Precursor feed rate (μmol/min)	Particle ratio (%)	Residence time (ms)	Deposition time (min)
1	Columnar	500	1.53	13	20	50
2	Granular	450	4.34	30	53	70
3	Branched	450	4.34	18	30	23

A field emission scanning electron microscope (FESEM, Nova 2300, FEI) and a transmission electron microscope (TEM, Spirit Lab6, FEI) were used for morphology and thickness characterization

of as-prepared films. The crystal structure of as-prepared TiO_2 films was characterized using an X-ray diffractomer (XRD, Geigerflex D-MAX-A, Rigaku, Tokyo, Japan) with Cu-Kα radiation at 35 kV and 35 mA. XRD patterns of columnar, granular, and branched structured films were scanned from 20° to 60° of 2θ. A UV-Vis spectroscope (Cary 100, Varian, Palo Alto, CA, USA) was used for absorption spectra of as-prepared films across the ultraviolet and visible light spectra. The bandgap energy of each film was obtained from their respective UV-Vis absorption spectra by plotting the correlation between photon energy (hv) and $(\alpha_{KM}hv)^{0.5}$. α_{KM} is the light absorption coefficient of the TiO_2 films calculated using the *Kubelka-Munk* formalism which is expressed as [24]:

$$\alpha_{KM} = \frac{(1-R_\infty)^2}{2R_\infty} \quad (1)$$

where R_∞ is the reflectance of an infinitely thick sample. Since TiO_2 is an indirect semiconductor, bandgap energy can be obtained from the linear correlation between the photon energy and the square root of the absorption coefficient [24].

2.2. Estimation of Surface Area of TiO_2 Films

The total surface area of each film type was estimated by mimetic methods. For the columnar film, a column was considered as a cone shape (Figure S1a) and the arrangement of columns on the film was assumed as the hexagonal packing of circles (Figure S1b). The granular structure was mimicked with two cases: granular film-1 and granular film-2 (Figure S1a). Granular film-1 was considered to be the arrangement of a single layer of small, primary particles on the lateral surface of a hexagonally packed column. Granular film-2 was assumed to be numerous hexagonally close-packed primary particle spheres within the boundary of the column (Figure S1c). In the case of the branched structure, the film was mimicked as cone-shaped columns with cone-shaped branches on their lateral surface as shown in Figure S1a. The cone-shaped branches on the lateral surface of the column were arranged as the hexagonal packing of circles (Figure S1b). Table S1 lists the dimensions for the deposited area of the film, the single column, the single primary particle and the single branch as determined from their photos and electron microscope images.

2.3. Culture and Sampling Cells

E. coli BL21 was cultured for 18 h in growth medium at 37 °C. Growth medium was prepared by dissolving 25 g of Luria-Bertani (LB) broth powder (LB broth, Difco) in 1 L of deionized (DI) water and autoclaving for 15 min at 121 °C. During culturing, the optical density at 600 nm (OD_{600}) of the culture solution was measured every hour to establish the onset of the stationary growth phase of *E. coli* growth (which corresponded to 1.4×10^9 cells/mL after 18 h of growth time).

The culture solution was sampled at t = 18 h and cells were pelleted by centrifugation for 10 min at 3000 rpm. Pelleted cells were suspended in 50 mL of buffer solution (5.0 mM sodium sulfate) creating a working cell suspension with a concentration of approximately 10^8 cells/mL. Viable *E. coli* concentration was determined from CFU (colony forming unit) plate counts: after serial dilutions, culture samples were plated on LB agar (Difco) followed by incubation for 12 h at 37 °C. Each sample was plated in triplicate.

2.4. Light and Material Control Tests

In order to determine the direct effect of light on *E. coli* viability, a light control was conducted. An arc Xe lamp (Oriel, Stratford, CT, USA) was used as the light source and was operated at 450 W. A water filter was attached to the lamp to remove infrared light. The *E. coli* solution was irradiated by the arc Xe lamp and 100 μL solution was sampled at 0, 30, 60, 90 and 120 min. In order to cut off ultra violet (UV) light (UVB and UVC), a blue band pass filter was attached and the effect of light on *E. coli* cells with and without the blue band pass filter was compared. In addition, the light intensity of the lamp was measured using a spectroradiometer (RPS900, International Light, Peabody, MA, USA) with and without the blue band pass filter to verify that it could effectively remove the strong UV wavelengths. UVB and UVC have been reported to inactivate some microorganisms [25]. Thus, in order to clearly investigate inactivation of *E. coli* by photocatalytic and photoelectrochemical reaction, the direct effect of UVB and UVC on *E. coli* should be minimized.

The effect of non-irradiated nanostructured TiO_2 films on *E. coli* viability was also examined. As-prepared TiO_2 film was immersed in the 50 mL *E. coli* solution and samples taken at 0, 30, 60, 90 and 120 min. A second material control experiment was conducted with 0.8 V of external voltage applied to the TiO_2 film to determine the effect of the TiO_2 film with electric bias. During the material control experiments, the reactor was covered with aluminum foil to block ambient light.

2.5. Photocatalytic and Photoelectrochemical Inactivation of E. coli

Figure 1. A schematic diagram of the experimental setup used for photocatalytic and photoelectrochemical inactivation of *E. coli*.

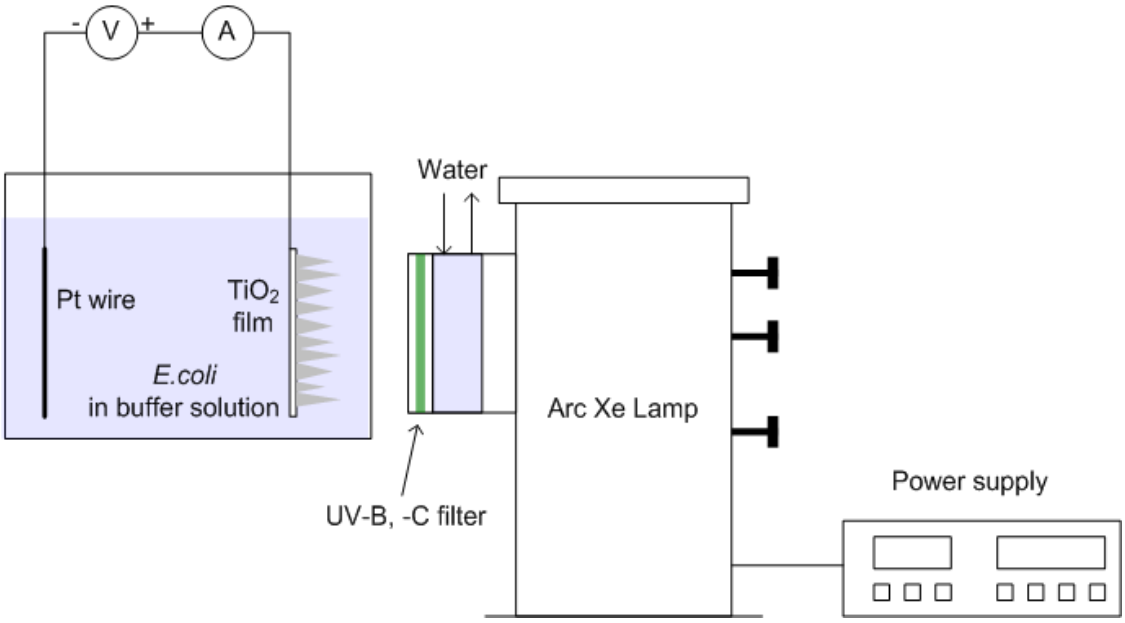

Photocatalytic and photoelectrochemical inactivation of *E. coli* was conducted as shown in Figure 1. For photocatalytic inactivation, only the TiO_2 film was immersed in the *E. coli* solution (no platinum wire was used). Both the TiO_2 film and the platinum (Pt) wire were immersed in solution while 0.8 V electric potential was applied between the two electrodes using a sourcemeter

(SourceMeter 2400, Keithley, Cleveland, OH, USA) for photoelectrochemical inactivation. The arc Xe lamp was used as the light source at 450 W with the water and the blue band pass filters in place. The intensity of UVA (315–400 nm) range of the lamp was 2.9 μW/cm^2. The *E. coli* solution in the inactivation reactor was sampled at 0, 5, 10, 15, 20, 30, 60 and 120 min. During *E. coli* inactivation, the culture was kept mixed by a magnetic stirrer. Experimental parameters of this study are summarized in Table 2.

Table 2. Summary of experimental parameters of inactivation for *E. coli*.

No.	Test	Objective	Experimental conditions
1	Light control test	Examine effect of light on viability of *E. coli* cells without TiO_2 films	Reactor volume: 50 mL
2	Material control test	Examine effect of TiO_2 films on viability of *E. coli* cells without irradiation of light	Initial active cell concentration (C_0): 10^8 cells/mL
3	Photocatalytic inactivation	Study inactivation of *E. coli* with TiO_2 films under irradiation of light without external voltage	Light source: 450 W arc Xe lamp
4	Photoelectrochemical inactivation	Study inactivation of *E. coli* with TiO_2 films under irradiation of light with external voltage	TiO_2 films: columnar, granular, and branched structure

3. Results and Discussion

Figure 2 shows SEM and TEM images of as-prepared columnar, granular, and branched TiO_2 films. In all cases, thickness of films was well controlled around 2 μm. In Figure 2a–c, it is shown that TiO_2 was well developed in one direction without any grains or branches. In addition, the tip of the single column was very sharp so that TiO_2 monomers or small primary particles deposited on the film were completely sintered and formed a single column. The granular structure was composed of numerous small grains (Figure 2d,e) while the branched structure had some sharp branches on its surface, which were composed of well-sintered grains (Figure 2g,h). TEM images of these structures more clearly depict this distinction (Figure 2f,i). In the case of granular TiO_2, small grains are observed whereas 1-D branches are shown in the branched TiO_2.

XRD patterns of as-prepared TiO_2 films are shown in Figure 3. For all morphologies, the anatase phase of TiO_2 was synthesized. The XRD pattern of the columnar TiO_2 film shows a peak only for the [112] direction of the anatase phase. This indicates that columns of the film were grown only in the preferred direction of [112]. On the other hand, the XRD pattern of the granular film matches well with the particle diffraction file (PDF) reference peak of the anatase phase and depicts numerous peak directions. This implies that the small grains composing the granular structure were randomly deposited and not well oriented. The XRD pattern of the branched TiO_2 film also closely matches the peaks from the PDF of anatase. However, the relative intensity of the peak of [101] direction was lower than that of the granular structure, possibly because the [101] direction from small primary particles initially deposited on the film was lost by sintering among them when forming branches.

Figure 2. Scanning electron microscopy (SEM) and transmission electron microscopy (TEM) images of (**a**), (**b**), (**c**) columnar, (**d**), (**e**), (**f**) granular and (**g**), (**h**), (**i**) branched TiO_2 films.

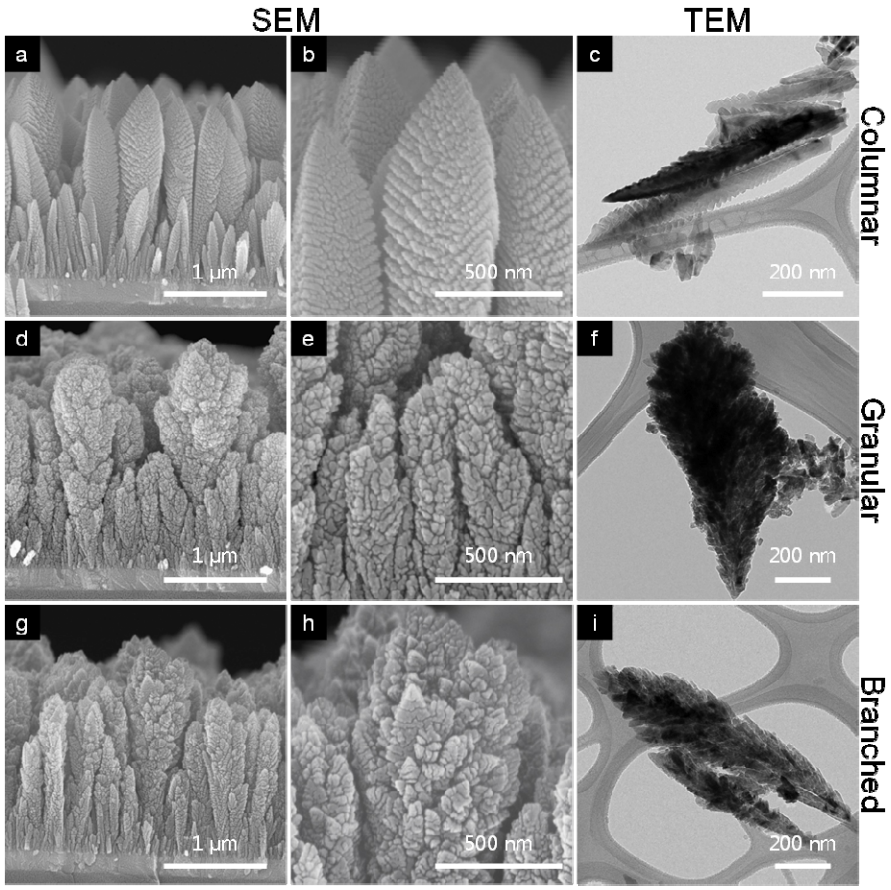

Figure 3. X-ray diffraction (XRD) patterns of columnar, granular, and branched TiO_2 films synthesized by ACVD. Black solid circles indicate peaks from Tin-doped Indium oxide (ITO) substrate.

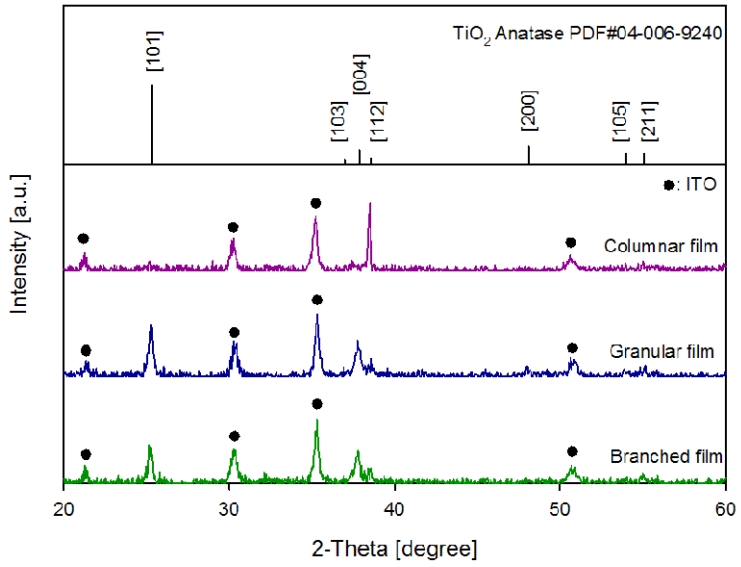

UV-Vis absorption spectra of the TiO_2 films are shown in Figure S2. In all films, the bandgap energy of TiO_2 was determined to be about 3.2 eV, which matches the reference bandgap energy of anatase TiO_2. This result means that all as-prepared films can be activated by light at wavelengths below 390 nm.

In Figure S3, measurement of light intensity of the arc Xe lamp shows that the blue band pass filter cuts off UVB and UVC. Although both UVB and UVC are completely removed with the filter, the filtered light still includes UVA, which can activate TiO_2 films to inactivate microbes.

Figure S4 shows the effect of irradiation light on the viability of *E. coli* with and without the blue band pass filter. While 10% of *E. coli* was inactivated after 2 h of irradiation with the filter in place, 99.999% of *E. coli* were killed within 30 min by irradiation of light without the filter. This result implies that UVB and UVC are lethal to *E. coli* cells whereas the effect of UVA is rather minimal over a period of two hours. Therefore, the blue band pass filter was attached to the lamp to minimize the effect of UVB and UVC light on the inactivation of *E. coli* cells when examining inactivation efficiency by photocatalytic and photoelectrochemical reactions. In addition, it was confirmed that TiO_2 itself does not have any effect on the inactivation of *E. coli* with and without external voltage in dark conditions. (Figure S5).

Results of photocatalytic and photoeletrochemical inactivation of *E. coli* using columnar, granular and branched TiO_2 films are shown in Figure 4. In all cases, the concentration of *E. coli* seems to exponentially decrease with respect to inactivation time. This indicates that inactivation of *E. coli* follows Chick's Law which says that the inactivation rate of bacteria can be expressed as a first ordered reaction with respect to the concentration of viable cells in a reactor [24]. According to Chick's Law, the inactivation rate can be given as follows:

$$Rate = \frac{dC_t}{dt} = -kC_t \tag{2}$$

where C_t is the active cell concentration at time t. From Equation (2) the inactivation rate constant can be obtained as Equation (3).

$$k = -\frac{\ln\frac{C_t}{C_0}}{t} \tag{3}$$

where the inactivation rate is normalized by the surface area of the films. The normalized rate can be obtained as follows:

$$Normalized\ Rate = \frac{1}{A}\frac{dC_t}{dt} = -k'C_t \tag{4}$$

where A is the surface area of the films and k' is the normalized rate constant.

$$k' = \frac{k}{A} \tag{5}$$

Figure 4. Photocatalytic and photoelectrochemical inactivation of *E. coli* using columnar, granular, and branched TiO_2 films. Error bars represent the standard deviation of triplicate measurements.

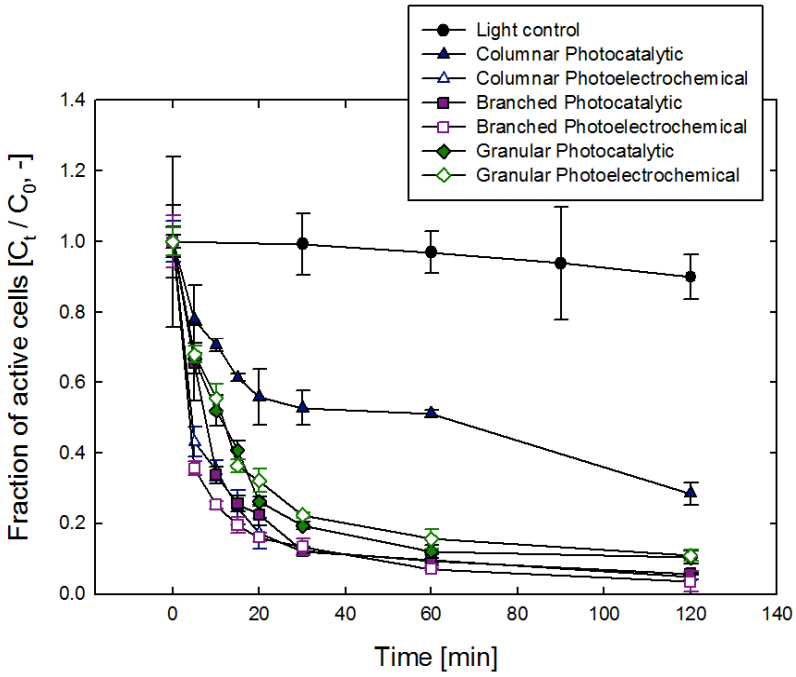

Since the initial concentration C_0 was fixed as 10^8 cells/mL, the inactivation rate constant can represent the inactivation efficiency by photocatalytic and photoelectrochemical reaction for each film morphology. The k value for each case was obtained from the linear slope of a log scale plot of photocatalytic and photoelectrochemical inactivation of *E. coli*. The inactivation rate constant, k for each case is shown in Figure 5.

Figure 5. Inactivation rate constant of photocatalytic and photoelectrochemical inactivation of *E. coli* using columnar, granular, and branched TiO_2 films.

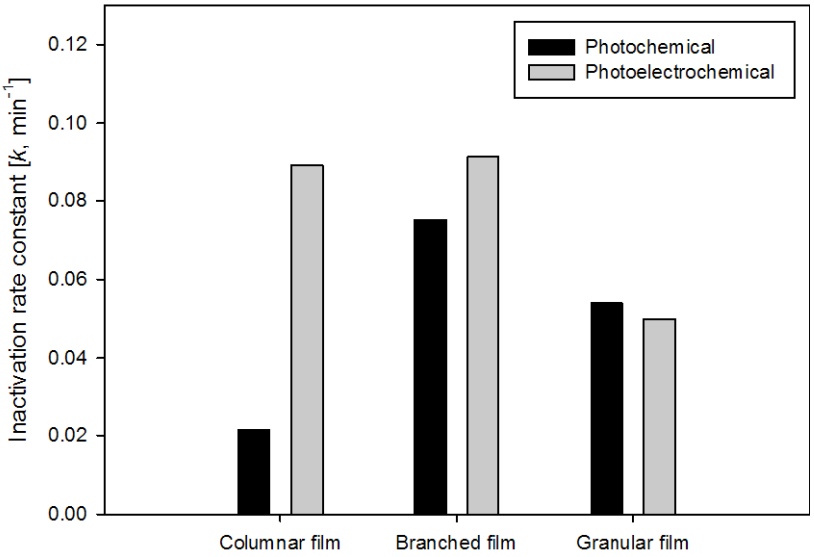

In the case of inactivation using the columnar TiO_2 film, the rate constant of photoelectrochemical inactivation was 330% higher than that of photocatalytic inactivation. This could be caused by a reduced electron-hole recombination rate due to enhancement of electron transfer to the cathode (platinum wire) through the column, which does not have any grain boundary effect (Figure 6).

Figure 6. Electron transfer through a columnar, a granular and a branched TiO_2 film.

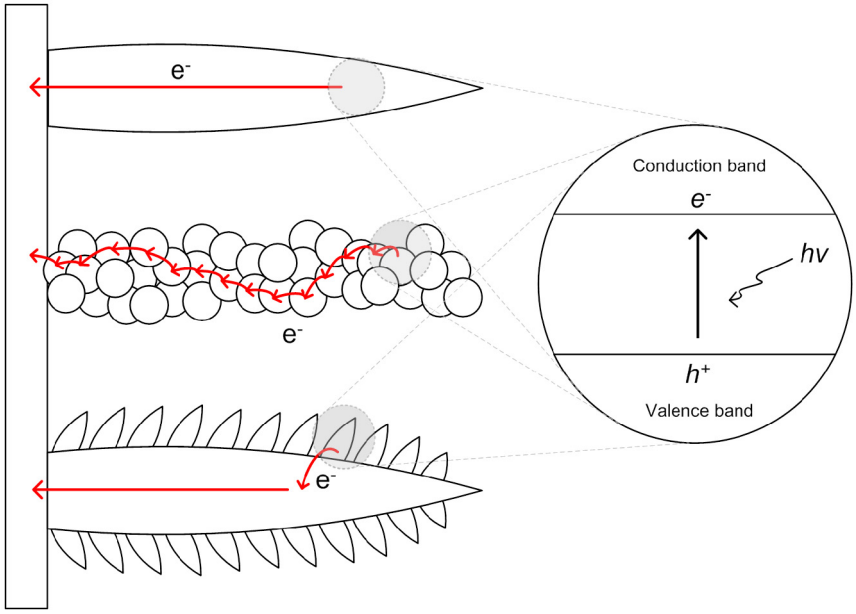

Thus, more electron-hole pairs could generate more reactive oxygen species, which could result in a higher inactivation rate of *E. coli*. On the other hand, the photoelectrochemical reaction rate constant by the branched TiO_2 film was only 30% higher than photocatalytic reaction rate constant. Although an applied voltage (0.8 V) between the anode (TiO_2 film) and the cathode (platinum wire) was able to promote separation of electron-hole pairs generated in the TiO_2, grain boundaries between branches and the main column could interrupt the fast transfer of electrons, consequently limiting the overall enhancement of the inactivation rate constant (Figure 6). In the case of the granular film, the photocatalytic and the photoelectrochemical rate constants were almost the same, which means that the electric bias could not enhance e-h separation in the film.

Table 3. Estimated surface area of TiO_2 films.

	Columnar film	**Granular film-1**	**Granular film-2**	**Branched film**
Total surface area of TiO_2 (m^2)	6.88×10^{-4}	3.18×10^{-3}	1.69×10^{-2}	6.34×10^{-3}
Normalized rate constant of PC [a] by surface area (k', $min^{-1} \cdot m^{-2}$)	31.1	16.9	3.2	11.8
Normalized rate constant of PEC [b] by surface area (k', $min^{-1} \cdot m^{-2}$)	129.4	15.7	2.9	14.4

[a] Photochemical inactivation; [b] Photoelectrochemical inactivation.

The surface area of the films could also significantly affect the inactivation rate. The larger surface area of TiO_2 can promote the release of electrons and holes from the TiO_2 film into the buffer solution generating reactive oxygen species. Eventually this could enhance inactivation rate. The photocatalytic reaction rate constants in Figure 5 exhibits this surface area effect for three different morphologies. No separation of electron-hole pairs by an applied electric potential occurred in the case of photocatalytic inactivation, therefore the rate constants could be affected by the surface area of the films. As shown in Figure 5, the photocatalytic inactivation rate constants of the branched and the granular TiO_2 film were 280% and 160% higher, respectively, than that of the columnar film. These larger inactivation rate constants reflect the fact that the branched film and the granular film (case of Granular film-1 in Table 3) have a 820% and 360% larger surface area, respectively, than the columnar film (Table 3).

Sunanda *et al.* [17] established a mechanism for inactivation of *E. coli* cells by reactive oxygen species that is generated by a photocatalyst. The reactive species such as hydroxyl radicals can oxidize and eventually destruct bacterial membrane and DNA strand, leading to cell lyses (release of metabolites, protein, and RNA from the cell [26]. Such an inactivation process breaks cellular structures. SEM images of the films support this mechanism (Figure S6), which show the top view of the columnar TiO_2 film before and after inactivation. In Figure S6b, the integrity of *E. coli* cells was destroyed and cellular biomaterials or cell debris "dissolved" on the surface of TiO_2 film.

Figure 7 shows the change in the inactivation rate constant obtained from a columnar film with respect to repeated use in 2-h photoelectrochemical inactivation trials. The inactivation rate initially decreased by about 22% between the first and second 2-h trial, with little drop-off observed in subsequent trials. The initial drop in inactivation rate could occur due to inactivated cell debris attached to the film surface as shown in Figure S6. These residual cells could block activation sites of the TiO_2 film. After time, the cell debris is eventually decomposed in the aqueous solution, allowing the inactivation rate to thereafter be sustained. The results demonstrate that the TiO_2 film is a sustainable material for the photocatalytic inactivation of *E. coli* in water.

Figure 7. Photoelectrochemical inactivation rate constant with respect to repeated inactivations.

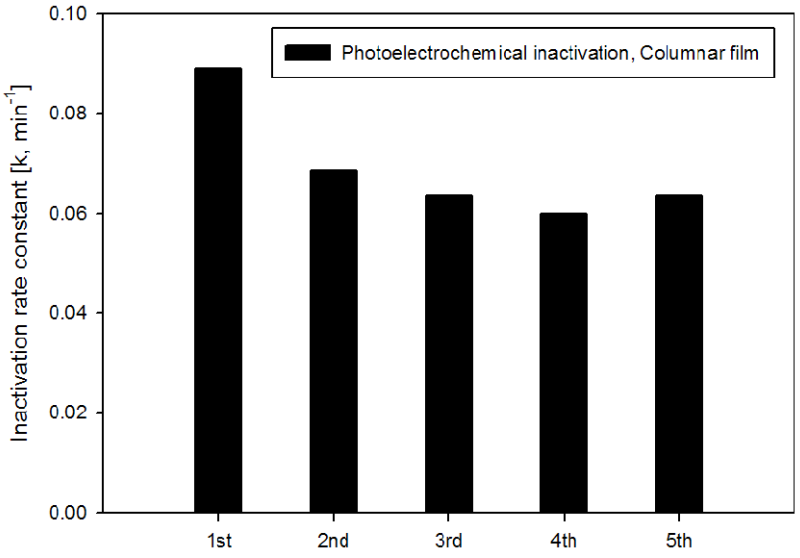

4. Conclusions

TiO_2 films with different morphologies—columnar, granular, and branched structures—were successfully synthesized via the ACVD method to inactivate *E. coli* in water. For all morphologies, the thickness was well controlled at about 2 μm and anatase phase films were obtained. *E. coli* is rapidly killed by UVB and UVC in the absence of the TiO_2 films, but most *E. coli* survives under UVA. The TiO_2 films did not have any bactericidal effects on *E. coli* in the dark condition whereas they inactivated *E. coli* cells strongly by photocatalytic and the photoelectrochemical reaction under UVA light. In the case of the columnar TiO_2 films, the photoelectrochemical inactivation rate was 330% higher than the purely photocatalytic inactivation rate. On the other hand, applying a potential bias to a branched TiO_2 film only increased the inactivation rate by 30%. In the case of the granular film, both inactivation rates were similar. The significant difference in the effectiveness of microbial inactivation between morphologies could be caused by different electron transfer rates through the TiO_2 films, which affects the recombination rate of e-h pairs generated by photoactivation. Moreover, the surface area of the TiO_2 films was another influential factor on microbial inactivation. The branched and the granular structure had a nine times and 2.5 times larger surface area than the columnar structure, respectively. The much larger surface area caused much faster inactivation of *E. coli* in the photocatalytic reaction. Finally, the TiO_2 film showed a sustained inactivation rate after repeated use for inactivation of microbes. Our UVA-based photosensitizers will potentially lead to an improvement of solar disinfection efficiency because the UVA spectrum is the dominant UV radiation in sunlight.

Acknowledgments

This study is partially supported by the Photosynthetic Antenna Research Center (PARC), an Energy Frontier Research Center funded by the U.S. Department of Energy, Office of Science, Office of Basic Energy Sciences under Award Number DE-SC 0001035. This work was also performed in part at the Nano Research Facility (NRF), a member of the National Nanotechnology Infrastructure Network (NNIN), which is supported by the National Science Foundation under Grant No. ECS-0335765. Any opinions, findings, conclusions, or recommendations expressed in this material are those of the author(s) and do not necessarily reflect the views of the National Science Foundation. NRF is part of the School of Engineering and Applied Science at Washington University in St. Louis.

Conflict of Interest

The authors declare no conflict of interest.

References

1. Shannon, M.A.; Bohn, P.W.; Elimelech, M.; Georgiadis, J.G.; Marinas, B.J.; Mayers, A.M. Science and technology for water purification in the coming decades. *Nature* **2008**, *452*, 301–310.
2. Montgomery, M.A.; Elimelech, M. Water and sanitation in developing countries: Including health in the equation. *Environ. Sci. Technol.* **2007**, *41*, 17–24.

3. Kemper, K.E. Groundwater-from development to management. *Hydrogeol. J.* **2003**, *12*, 3–5.
4. Szewzyk, U.; Szewzyk, R.; Manz, W.; Schleifer, K.H. Microbiological safety of drinking water. *Annu. Rev. Microbiol.* **2000**, *54*, 81–127.
5. Gopal, K.; Tripathy, S.S.; Bersillon, J.L.; Dubey, S.P. Chlorination byproducts, their toxicodynamics and removal from drinking water. *J. Hazard. Mater.* **2007**, *140*, 1–6.
6. Krasner, S.W.; Weinberg, H.S.; Richardson, S.D.; Pastor, S.J.; Chinn, R.; Sclimenti, M.J.; Onstad, G.D.; Thruston, A.D. Occurrence of a new generation of disinfection byproducts. *Environ. Sci. Technol.* **2006**, *40*, 7175–7185.
7. Zhang, D.; Li, G.; Yu, J.C. Inorganic materials for photocatalytic water disinfection. *J. Mater. Chem.* **2010**, *20*, 4529–4536.
8. Matsunaga, T.; Tomoda, R.; Nakajima, T.; Wake, H. Photoelectrochemical sterilization of microbial cells by semiconductor powders. *FEMS Microbiol. Lett.***1985**, *29*, 211–214.
9. Wei, C.; Lin, W.Y.; Zaina, Z.; Williams, N.E.; Zhu, K.; Kruzic, A.P.; Smith, R.L.; Rajeshwar, K. Bactericidal activity of TiO_2 photocatalyst in aqueous media: toward a solar-assisted water disinfection system. *Environ. Sci. Technol.* **1994**, *28*, 934–938.
10. Hu, C.; Lan, Y.; Qu, J.; Hu, X.; Wang, A. $Ag/AgBr/TiO_2$ visible light photocatalyst for destruction of azodyes and bacteria. *J. Phys. Chem. B* **2006**, *110*, 4066–4072.
11. Hu, C.; Guo, J.; Qu, J.; Hu, X. Photocatalytic degradation of pathogenic bacteria with AgI/TiO_2 under visible light irradiation. *Langmuir* **2007**, *23*, 4982–4987.
12. Wu, B.; Zhuang, W.Q.; Sahu, M.; Biswas, P.; Tang, Y.J. Cu-doped TiO(2) nanoparticles enhance survival of *Shewanella oneidensis* MR-1 under ultraviolet light (UV) exposure. *Sci. Total Environ.* **2011**, *409*, 4635–4639.
13. Wang, P.; Huang, B.; Qin, X.; Zhang, X.; Dai, Y.; Whangbo, M.H. $Ag/AgBr/WO_3$ $3H_2O$: Visible-light photocatalyst for bacteria destruction. *Inorg. Chem.* **2009**, *48*, 10697–10702.
14. Mccullagh, C.; Robertson, J.M.C.; Bahnemann, D.W.; Robertson, P.K.J. The application of TiO_2 photocatalysis for disinfection of water contaminated with pathogenic micro-organisms: A review. *Res. Chem. Intermed.* **2007**, *33*, 359–375.
15. Amezaga-Madrid, P.; Nevarez-Moorillon, G.V.; Orrantia-Borunda, E.; Miki-Yoshida, M. Photoinduced bactericidal activity against *Pseudomonas aeruginosa* by TiO_2 based thin films. *FEMS Microbiol. Lett.* **2002**, *211*, 183–188.
16. Kuhn, K.P.; Chaberny, I.F.; Massholder, K.; Stickler, M.; Benz, V.W.; Sonntag, H.G.; Erdinger, L. Disinfection of surfaces by photocatalytic oxidation with titanium dioxide and UVA light. *Chemosphere* **2003**, *53*, 71–77.
17. Sunada, K.; Watanabe, T.; Hashimoto, K. Studies on photokilling of bacteria on TiO_2 thin film. *J. Photochem. Photobiol. A* **2003**, *156*, 227–233.
18. Reddy, M.P.; Phil, H.H.; Subrahmanyam, M. Photocatalytic disinfection of *Escherichia coli* over titanium (IV) oxide supported on Hβ zeolite. *Catal. Lett.* **2008**, *123*, 56–64.
19. Yu, H.; Quan, X.; Zhang, Y.; Ma, N.; Chen, S.; Zhao, H. Electrochemically assisted photocatalytic inactivation of *Escherichia coli* under visible light using a $ZnIn_2S_4$ film electrode. *Langmuir* **2008**, *24*, 7599–7604.
20. Hayden, S.C.; Allam, N.K.; El-Sayed, M.A. TiO_2 Nanotube/CdS hybrid electrodes: Extraordinary enhancement in the inactivation of *Escherichia coli*. *J. Am. Chem. Soc.* **2010**, *132*, 14406–14408.

21. Thimsen, E.; Rastgar, N.; Biswas, P. Nanostructured TiO_2 films with controlled morphology synthesized in a single step process: Performance of dye-sensitized solar cells and photo watersplitting. *J. Phys. Chem. C* **2008**, *112*, 4134–4140.
22. An, W.J.; Thimsen, E.; Biswas, P. Aerosol-chemical vapor deposition method for synthesis of nanostructured metal oxide thin films with controlled morphology. *J. Phys. Chem. Lett.* **2010**, *1*, 249–253.
23. An, W.J.; Jiang, D.D.; Matthews, J.R.; Borrelli, N.F.; Biswas, P. Thermal conduction effects impacting morphology during synthesis of columnar nanostructured TiO_2 thin films. *J. Mater. Chem.* **2011**, *21*, 7913–7921.
24. Reyes-Coronado, D.; Rodriguez-Gattorno, G.; Espinosa-Pesqueira, M.E.; Cab, C.; Coss, R.; Oskam, G. Phase-pure TiO_2 nanoparticles: anatase, brookite and rutile. *Nanotechnology* **2008**, *19*, doi:10.1088/0957-4484/19/14/145605.
25. Chang, J.C.; Ossoff, S.F.; Lobe, D.C.; Dorfman, M.H.; Dumais, C.M.; Qualls, R.G.; Johnson, J.D. UV inactivation of pathogenic and indicator microorganisms. *Appl. Environ. Microbiol.* **1985**, *49*, 1361–1365.
26. McGuigan, K.G.; Joyce, T.M.; Conroy, R.M. Solar disinfection: use of sunlight to decontaminate drinking water in developing countries. *J. Med. Microbiol.* **1999**, *48*, 785–787.